MULTIDISCIPLINE ANALYSIS OF A FATAL LPG TANK RUPTURE

Bernard Ross
Failure Analysis Associates
149 Commonwealth Drive
Menlo Park, California 94025

Clifford Lange
Novellus Systems
3011 N. First Street
San Jose, California 95134

Jeffrey Eischen
Department of Mechanical & Aerospace Engineering
North Carolina State University
Box 7910
Raleigh, North Carolina 27695

Abstract: An LPG tank fabricated by a major manufacturer in the late 1940s with rolled skid plate, commonly used in steel floor construction, burst catastrophically under direct sunlight. The rupture caused extensive property damage and fatal injury. Metallurgical analysis revealed that at time of fabrication the full penetration longitudinal seam weld of the tank had been torch cut and then reconnected with only an external partial penetration weld. In consequence, a full-length axial crack was introduced in the tank shell. Moreover, the rewelding was poor with rampant porosity slag deposits and lack of homogeneity. Prominent weld flaws were identified as singular origins of the burst fracture.

A variety of analytical techniques were undertaken to develop the etiology of failure. First, a maximum equivalent stress failure criterion was applied to determine the nominal rupture pressure for the tank. Discontinuity stresses at the elliptical heads were acknowledged in the stress analysis. Next, an extensive fracture mechanics study which accounted for the combined effects of lack of penetration and discrete flaws in the longitudinal weld seam was performed. The presence of a flaw embedded in a cylinder with a semi-infinite axial crack presented a unique geometry not easily modeled by normal solutions.

A series of burst tests was carried out under hydrostatic loading using exemplar propane tanks fabricated with an analogous partial penetration seam weld. Results of those tests including burst pressures, depth of weld penetration, fracture mode, and material hardness were extrapolated to determine the critical pressure. A minimum rupture pressure of 535 psi was calculated for the accident tank which under proper construction should have manifested a burst pressure of 1600 psi.

A thermodynamics study of the two-phase liquid-vapor propane system was performed. This work established circumstantially that the LPG tank was necessarily overfilled to the 93% level, vis-à-vis the standard 80% requirement. Under this condition, the requisite burst pressures could be achieved at prevailing tank surface temperatures because the LPG contents were in the saturated liquid phase. Concomitantly, it was established through bench testing that the 40-year-old pressure relief valve (safety valve) was frozen due to severe environmental rusting.

Key Words: Fracture mechanics; Propane tank burst, Stress analysis, Temperature effects

The Accident: This serious fatal accident occurred at a scrap metal junkyard and involved a live-in house trailer with appliances fired by liquid propane (LPG) contained in an ASME designation tank which was resting freely on the towbar tongue of the trailer. This tank was unsuitable for these purposes since a DOT regulation LPG tank is required for trailer home appliances service, (stove, water heater, furnace) whilst the ASME tank is typically installed on LPG powered vehicles (taxis, forklifts, etc.) The accident occurred in early spring on a clear sunny California day with ambient temperatures in the low 80°F. range. The tank exterior was rusted black metal and could easily experience temperatures in direct sunlight as much as 30° - 40° above ambient.

Two large bangs were heard by surviving occupants of the trailer. Obviously, the first bang was rupture of the tank, and the second bang, deflagration of the released propane cloud which readily found source(s) of ignition according to Murphy's Law. The unsecured tank took off as a jet powered projectile and smashed into a nearby flat bed truck causing the combination vapor discharge hand valve with integral pressure relief valve to be broken off traumatically at its threaded connection with the tank. The layout of the accident scene is shown in Figure 1.

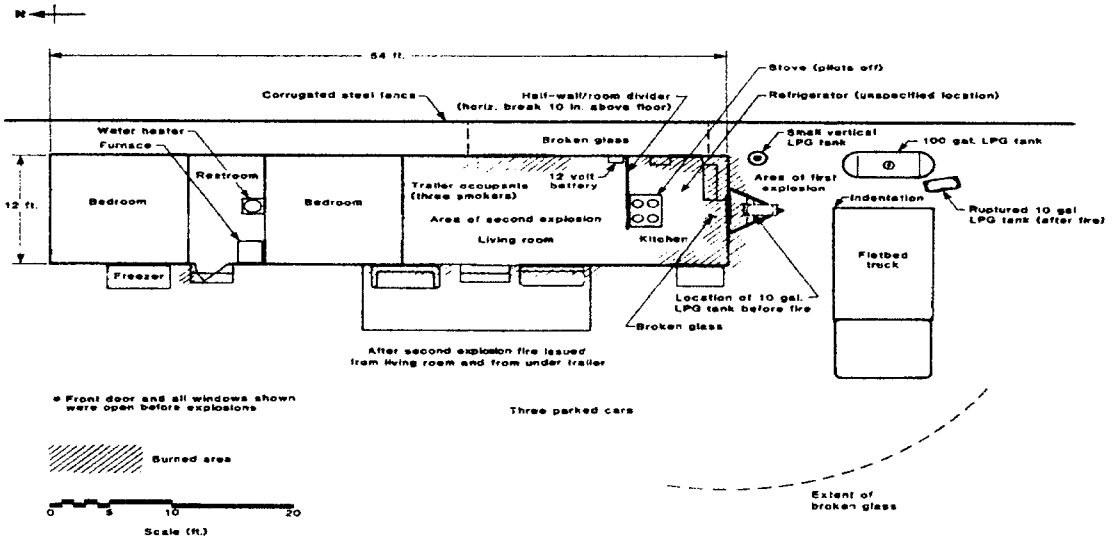

Figure 1: Accident Scene

Metallurgical Examination: The burst tank is shown in the two views of Figure 2. The ASME code plate indicated the tank was built in 1949. For some reason, the tank was fabricated from ordinary rolled steel diamond pattern skid plate (the lawyers salivate!). The tank fractured along its single longitudinal welded seam and the crack progressed into both ellipsoidal end caps (domes).

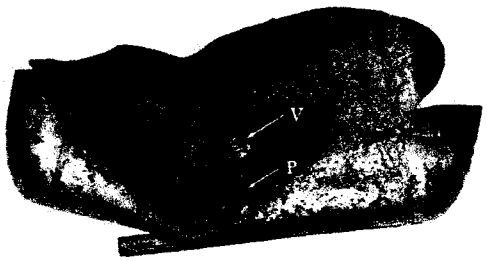

Location of the broken valve at V and the ASME code plate at P.

Rupture along the longitudinal weld at L and into the heads.

Figure 2: Views of the ruptured tank as received.

Closer views of a typical portion from the longitudinal fracture surface are shown in Figure 3. An amazing feature of the tank fabrication process was realization through visual and metallographic means that the cylindrical tank had been formed with a full penetration internal weld initially and then the weld was cut with a torch whence the tank shell was rerolled and rejoined with a shallow partial penetration external weld. (The ASME pressure vessel code requires a full penetration double weld.) This successor weld contained slag deposits, inclusions, lack of fusion, and rampant porosity. The bi-lateral welded joint structure can be discerned in Figure 3b. The fracture path also demonstrated a singular anomaly in form of a weld start-stop point as seen in Figure 4. A typical metallographical cross section of the failed joint is seen in Figure 5. The fracture plane manifests mainly brittle transgranular cleavage with little to no shear lip. Measurements of the fracture geometry indicated that the skid plate nominal thickness was 0.165 in. and the nonwelded portion (i.e., torch cut) or notch depth was typically 0.057 in.

(a) Magnification: ~1.5X

(b) Magnification: 3.65X

Figure 3: Closer views of the fracture face. Note the parallel contours from torch cutting (T) and welding slag (S) at the inner edge of the fracture. The fracture (C) is only 0.095" wide in some areas and a shear lip is absent at the inner edge and in segments of the outer edge.

Material identification was obtained through standard laboratory chemistry. In particular, tensile strength was determined through correlation with Knoop and Vickers microhardness readings. Normally the material strength properties would be confirmed with tests on a tensile specimen but such effort was precluded by the court since the failed tank was evidence in a litigation proceeding. The average values determined for ultimate tensile strength were 67-70 ksi for the plain carbon steel identified as being comparable to A36 plate (tank) and 89-103 ksi for the shielded metal arc weld material. The domes were made of SA414G steel.

Figure 4. Inner surfaces of coupons showing the fracture deviation around a weld stop/start point.

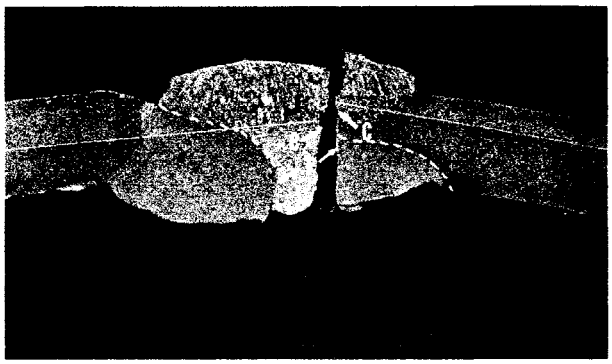

Figure 5. Metallographic Section. The original weld deposit (regions below dashed lines) was cut through producing the characteristic straight surfaces shown in profile at the arrows T.

The outage, or so-called 80%, tube projection into the tank appeared to be corroded and shorter than normal. A circular opening was milled out of the shell opposite this tube to gain better access. Measurement of the tube revealed that it was only 1-1/4 in. long instead of the design value of 2-5/8 in.

Bench tests were performed on the smashed discharge valve to ascertain condition of the pressure relief valve. Compressed nitrogen gas was used as the appropriate density fluid. Tests revealed that the valve leaked due to traumatic damages and the pressure relief valve was frozen due to its badly rusted condition. In this context, charactertistic pressures for the LPG tank and its hardware are $P_{WORKING}$ = 250 psi, P_{RELIEF} = 275 psi @ 130°F and $P_{HYDROTEST}$ = 375 psi.

Stress Analysis: The nominal longitudinal and circumferential (hoop) stresses in both the cylindrical portion of the tank and at the ends where the semi elliptical heads are joined were calculated by conventional means for pressure vessel analysis. In latter regard, the self-equilibrating (Saint Venant) discontinuity stresses were obtained from the following equations for the tank configuration sketched below.

$$\sigma_x = \frac{pa}{2t_o}\left[1 + \frac{6\beta^2 Da^3}{Et_0^2 b^2} e^{-\beta x} \sin \beta x\right]$$

$$\sigma_\theta = \frac{pa}{t_o}\left[1 - \frac{a^2}{4b^2} e^{-\beta x} \cos \beta x + \frac{3\beta^2 Da^3}{Et_0^2 b^2} \nu e^{-\beta x} \sin \beta x\right]$$

$$\sigma_{eq} = \left[\frac{1}{2}\left(\sigma_\theta - \sigma_x\right)^2 + \sigma_\theta^{\,2} + \sigma_x^{\,2}\right]^{\frac{1}{2}}$$

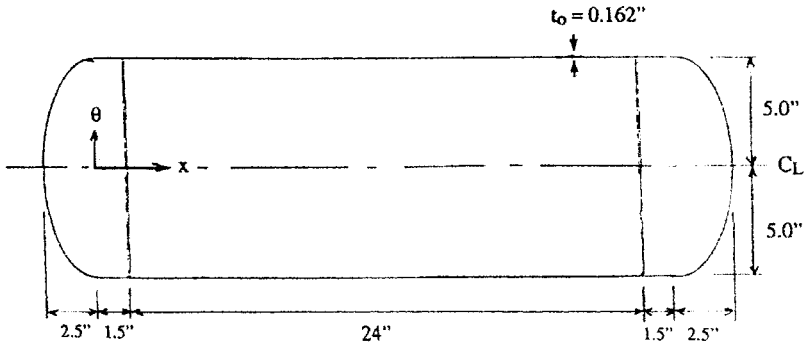

Geometry of Tank

Results of these calculations are presented in terms of the nondimensional stress-to-tank pressure ratio and shown in Figure 6. An interesting feature of the discontinuity stress profiles is fact that they attain maximum value(s) at a standoff distance from the circumferential joint (i.e., interface) itself. The curve for σ_{eq} in the plot represents the Von Mises equivalent stress which quantity is normally used in conventional failure analysis for a ductile material. A value of σ_{eq} = 30.95 p at 0.87 in. distance from the cylinder-dome interface was determined.

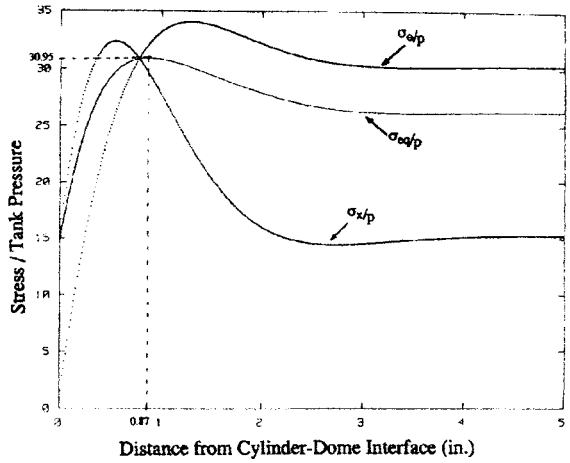

Figure 6: Nominal (full penetration) Stress Profiles for LPG Tank

Using the tensile strength value realized for the steel skid plate tank material and the Von Mises failure criterion, an as-designed burst pressure of 1615 psi was predicted. Here the material strength criterion used for failure was the flow stress; that is, the average stress between Tresca yield (0.5 σ_{ult}) and ultimate tensile strength (σ_{ult}). A flow stress value of 50 ksi was obtained for the **tank** shell.

An ancillary calculation was carried out whereby the primary tensile separation (membrane) and secondary moment (bending) effects on the weld seam due to internal pressure acting on the longtiudinal flame cut notch opposing faces were acknowledged. Only the weld ligament thickness (i.e., 0.105 in.) was assumed to be stressed. The resultant numerical calculations indicated that σ_{eq} = 46.05 p at x = 1.15 in. For a **weld** flow stress of 72 ksi, the predicted burst pressure was 1565 psi. In this particular case, the membrane stresses were tensile and adverse, however, the secondary bending stresses were beneficial since they are compressive at the crack root.

Fracture Mechanics Analysis: A Linear Elastic Fracture Mechanics (LEFM) analysis was performed to determine the burst pressure required to initiate brittle fracture of the seam weld in the tank. LEFM requires the computation of an applied Stress Intensity Factor, K_I, determined from geometry of the structure and mode of loading. The present geometry is a cylindrical shell with a full-length longitudinal (axial) crack and the uniform loading is due to internal pressure. Once obtained, the applied stress intensity factor, K_I, is compared to the fracture toughness, K_{IC}, of the tank material to determine if failure will occur.

The stress intensity factor for a cylinder with a two-dimensional axial crack subjected to internal pressure is dependent upon the radius to thickness ratio, R/t, of the cylinder. The present tank has a R/t ratio of 30. A search of existing K_I solutions revealed that the largest R/t ratio for which K_I solutions exist is 20. However, as a cylinder becomes larger in diameter and thinner in wall thickness the effects of curvature become less significant. In the limit, as $R/t \rightarrow \infty$, the stress intensity factor is identical to that for an infinitely long strip of finite width with a single edge crack. This concept is illustrated graphically in Figure 7. The strip solution for K_I provides an upper bound for the cylinder solutions and therefore a lower bound on burst pressure.

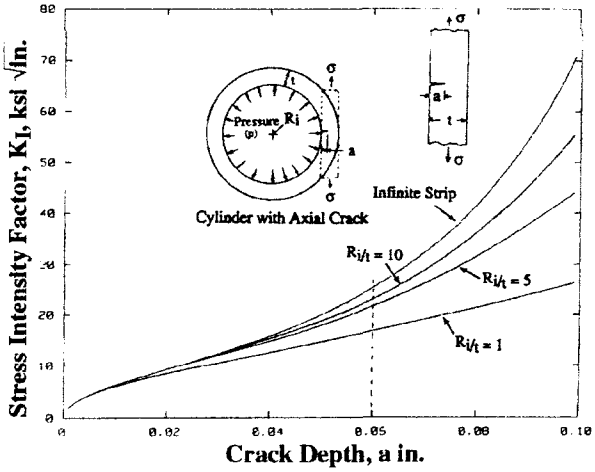

Figure 7: Stress Intensity Factor, K_I, for Cylinder with Axial Crack

For the tank at issue, the smallest weld penetration was 0.105 in. With a nominal wall thickness of 0.162 in., the deepest crack would be 0.057 in. Figure 7 shows that for crack depths up to 0.060in. the strip K_I solution provides a reasonable estimate (within 10%) of the cylinder K_I solutions for $R/t > 10$ without being overly conservative.

The K_I solution for an infinite strip of finite width with a single edge crack is:
$K_I = \sigma\sqrt{\pi a}F(a/b)$ a = crack depth (i.e., lack of penetration); b = width of strip (i.e. weld depth) σ = applied membrane stress From Figure 7, the stress intensity-pressure ratio factor for an approximate 0.06 in crack is $K_I/p=30$. The function F(a/b) is evaluated for the present geometry using data from the single edge notch solution found in any fracture mechanics handbook. Here, F(A/b) = 1.879. The effect of uniform pressure acting on the edges of the crack faces can be included into the K_I solution by simply adding the pressure, p, to the remotely applied membrane stress, σ, for an infinite strip. Including pressure on the crack faces in the K_I solution yields.

$$K_I = (30p + p)\sqrt{\pi(.057)} \bullet 1.879$$

$$K_I = 24.65p$$

References on the fracture properties of materials indicates that a fracture toughness of 20 ksi $\sqrt{in}$ constitutes a lower bound envelope for virtually all steels. Substitution of this value in the relationship above yields the burst pressure due to brittle fracture of the weld seam; that is, $\boldsymbol{P}$ = 811 psi.

The pressure computed for failure above does not include the increase in local circumferential stress due to the ellipsoidal domes at each end of the tank. Here, the bending component of hoop stress produces tension on the outside of the tank and tends to close the crack on the inner surface thus lowering the applied K_I. On the other hand, the membrane hoop stress is larger and it increases the applied K_I. In order to investigate the relative influence of circumferential membrane and bending stresses near the ellipsoidal domes, a K_I solution for far field bending (as opposed to tension) of an infinite strip was employed.

Redoing the previous calculations under these conditions resulted in an applied stress intensity factor-pressure ratio of 26.13 at a distance 1.87 in. from the cylinder-dome interface. Introducing the material fracture toughness value of 20 $K_{SI}\sqrt{in}$ yields a burst pressure of **P** = 765 psi. This rupture pressure was considered a lower bound because of conservative approximations employed in the analysis such as the beneficial effect of cylinder curvature, estimated to be about 6%.

The present failure analysis was refined further by considering the superposition of solutions for the lack-of-weld penetration full length axial notch and an embedded finite width flaw modeled as either a semicircle or ellipse. As before, the infinite strip solution can also be used to bound the K_I solution for the seam weld of the LPG tank with lack of penetration and an initial flaw. One such approximation is to extend the full length axial crack to include the entire leading edge flaw depth. However, since the finite strip solution is only two dimensional, no benefit is realized from the uncracked regions on either side of the flaw. This simulation unrealistically reduces the rupture pressure.

In order to include the uncracked regions on either side of the flaw in the stress intensity factor (K_I) solution, a method described by J.R. Rice was used. This approach enabled the change in stress intensity, ΔK, due to a corresponding variation in the crack front (i.e. the flaw) to be computed. The problem was formulated in general terms using a first order variation crack depth for the half-plane crack in an infinite body. A complete analysis based on the Rice theory which involved complex integral equations, yielded the applied stress intensity relation at the deepest part of the flaw; in particular, $K_I = \underline{3}4.4p$. Using the fracture toughness determined in the test program K_{IC} of 18.5 ksi $\sqrt{in}$ allowed the prediction of burst pressure as **P**=537 psi.

Test Program: Tests were performed to complement the analytical investigation. Three exemplar tanks were fabricated from low carbon steel floor plate (with a non-skid raised diamond pattern on one surface). The rolled cylinder was closed with a longitudinal weld seam placed on the ID side. This seam was then flame-cut and re-welded from the outside. The degree of weld bead penetration varied from complete to partial for the three-exemplar tanks. The domes were performed, made of SA414G carbon steel, and welded onto the cylindrical section with a circumferential OD seam and backing ring on the ID side. All joints were welded by the shielded metal arc (SMAW) technique (i.e., manual "stick welding"). A manual plunger pump was used to pressurize the exemplar tanks. Pressure was measured continuously by an Amot transducer with Vishay signal conditioner/amplifier instrumentation and recorded on an HP strip chart recorder. Each cylinder was hydrostatically loaded to failure, then the fracture zone was sectioned to

determine the longitudinal seam weld depth, wall thickness and hardness. Samples were removed from the fracture zone for comparison with the accident cylinder.

Failure in Tank #1 occurred at a maximum pressure of 1740 psig, in good agreement with the calculated value of 1616 psig based on a full penetration weld. The depth of fusion and wall thickness were measured in the rupture zone. Fusion depth ranged between 0.175 – 0.280 in. and wall thickness between 0.167 and 0.168 in. Brittle fracture (cleavage) was the predominant failure mode for Tank #1 with some ductile fracture seen near the outside surface as a narrow shear lip. Tank #2 failed in the weld at a maximum pressure of 1000 psig. Fusion depth ranged between 0.115 – 0.203 in. and wall thickness between 0.170 – 0.174 in. Brittle fracture (cleavage) was the predominant failure mode for Tank #2 but a portion of the cross section failed in a ductile mode as confirmed by a wide shear lip. A maximum pressure of 900 psig was recorded for Tank #3 at failure. Fusion depth ranged between 0.065 – 0.100 in. and wall thickness between 0.160 – 0.162 in. The fusion depth of this tank was less than that of the accident tank (i.e., 0.105-in. to 0.122-in.). Ductile fracture (shear) was the predominant failure mode for Tank #3 with a small portion of the cross section failing in a brittle mode. The notch-like stress concentration transition from the flame-cut surface to the load-bearing weld was visible in each tank failure.

Analysis of Test Results: An analysis was performed to extrapolate the burst pressure for the accident tank using results obtained from the hydrostatically tested exemplar tanks. The applied stress intensity factor, K_I, at failure was computed for each exemplar tank. This factor was actually representative of material fracture toughness since it was computed from the burst pressure. Because fracture toughness is related to fracture mode (brittle vs. ductile), an empirical relationship between the fracture toughness and percent flat fracture could be established. The percent flat fracture of the accident tank was assessed and a corresponding fracture toughness assigned based on the empirical relationship determined from the exemplar tank fracture surfaces. Equating the fracture toughness so determined to an applied value of K_I allowed a burst pressure for the accident tank to be computed. The procedure was valid because the weld ligaments in the exemplar tanks had flaws similar to those in the accident tank and therefore would manifest similar behavior.

The test burst pressure of 1740 psi for exemplar Tank #1 which had an external weld fusion thickness greater than the shell plate thickness (i.e., 0.175 0.280 in. vs. 0.167), agreed very well with the calculated nominal burst pressure of 1616 psi, for the tank with full penetration weld. Tanks #2 and #3 were deliberately fabricated with partial penetration welds (i.e., notched seams). Thus, a fracture mechanics analysis was needed.

The infinite strip solution used to compute the applied K_I for the accident tank was appropriate because the accident tank welded seam had very little crown and moderate (more than half of the base plate thickness) weld penetration. However, the infinite strip solution was not readily applicable to a fracture mechanics analysis of exemplar Tanks #2 and #3. As it turned out, due to fabrication difficulties, the weld crowns of the exemplar tanks contained most of the weld penetration, especially for Tank #3. Thus, for exemplar Tanks #2 and #3 a "remaining ligament" stress intensity factor solution was better suited to compute the applied values for K_I.

The remaining ligament (as opposed to a single edge crack) solution for K_I is found readily in the literature

$$K_I = 1.297 \frac{P}{\sqrt{\pi d}}$$

This relation was obtained through integral transform and is due to Stallybrass (1971). In terms of pressure (where P = pR), and weld depth (d), the expression becomes

$$K_I = 7.318\frac{p}{\sqrt{d}}$$

Using the test data for burst pressure, p, and depth of weld penetration, d, the values of K_I for Tanks #2 and #3 were calculated to be:

$K_I = 18.7\ ksi\ \sqrt{in}$. (80% flat fracture) for Tank #2 and $K_I = 23.4\ ksi\ \sqrt{in}$. (5% flat fracture) for Tank #3 respectively. These data points are represented in the plot of Figure 8.

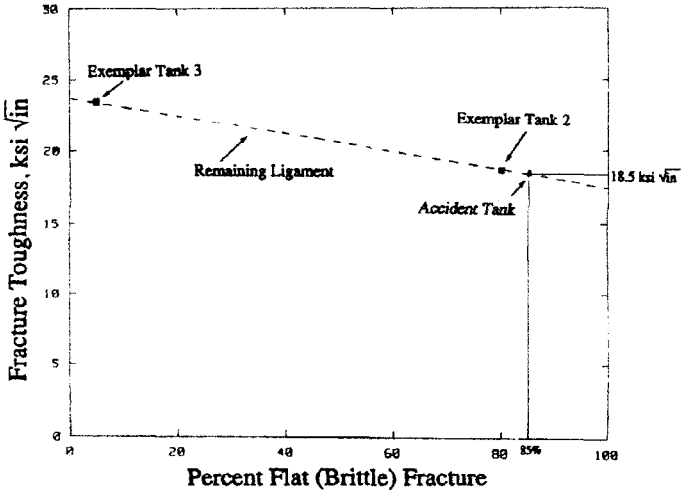

Figure 8. Fracture Toughness vs. Fracture Mode

The ensuing linear empirical relationship between fracture toughness and percent flat fracture enabled a prediction for burst pressure of the accident tank. Specifically, an 85% flat fracture topology was ascribed to the burst accident tank based on visual observation of SEM photographs. Reference to the test data plot of Figure 8 indicates that for 85% flat fracture a K_{IC} value of 18.5 ksi is predicted for the accident tank fracture toughness. However, the remaining ligament solution was not appropriate for the accident tank since it did not contain the significant weld crown of the shop fabricated exemplar tanks. Therefore, the previously mentioned single edge crack in an infinite strip solution was invoked. Apropos, the governing relation for stress intensity factor as a function of pressure became $K_I = 22.8p$ for an average crack depth of 0.054 in. which, in turn, implied a burst pressure of P = 811 psi.

Temperature-Pressure Behavior of Propane: The thermodynamic relationships between temperature, pressure, and volume for propane were obtained from a reference handbook. These relationships are presented in Figure 9 as a Temperature vs. Specific Volume diagram with lines of constant pressures as a parametric variable. Figure 9 shows the three phases of propane; namely, saturated liquid-vapor, saturated liquid and superheated vapor. To the left of the saturated liquid line, and below the critical temperature, propane is a compressed liquid.

Liquid propane tanks are designed to store their contents under saturated conditions. This condition is easily achieved because propane vaporizes at minus 43.7°F at 1 atmosphere (14.7 psi). When a LPG tank is subjected to change in temperature, the propane responds with a change in vapor pressure. For example, consider a tank of liquid propane at 70°F,

the vapor above the liquid will be at the saturation pressure, 124.3 psi (Figure 9). As the temperature increases to 130°F, some of the liquid propane boils to raise the vapor pressure while vapor also condenses due to the increased pressure. The equilibrium point is the saturation pressure for propane at 130°F (i.e., the maximum rated operating pressure) which turns out to be 274.5°F (i.e., the relief valve setting).

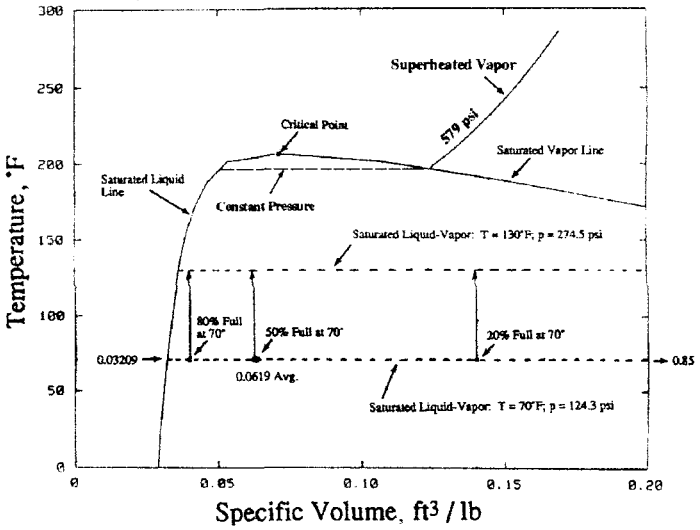

Figure 9. Temperature-Volume Diagram for Propane

An important observation is that as the initial volume of liquid propane in the tank increases (i.e., average specific volume decreases), the danger of exiting the saturated liquid-vapor phase and entering the compressed liquid phase becomes possible. It is for this reason that LPG tanks should not be filled over 80% capacity. In the saturated liquid region, small changes in temperature can result in large changes in pressure. To portray the potential rise in pressure that can occur from overfilling (i.e., more than 80%) an LPG tank and then subjecting the tank to temperature increase, the compressed liquid region for propane is expanded in Figure 10. The pressures attained when the temperature increases to 110°F (i.e., approximate surface temperature when tank exploded) are shown.

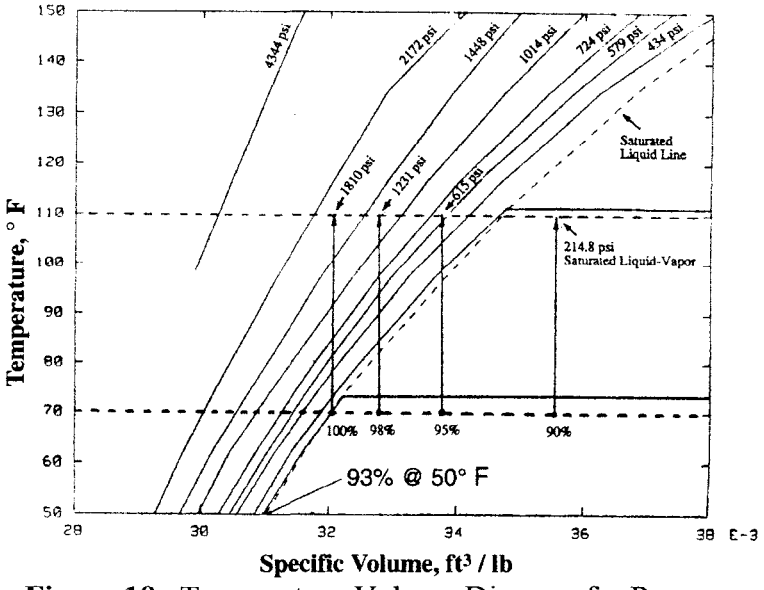

Figure 10. Temperature-Volume Diagram for Propane

Figure 10 demonstrates that if the tank were initially filled to 95% capacity at 70°F and the temperature increased to 110°F, the propane would become a compressed liquid and a pressure of 615 psi could be realized. However, when an LPG tank is overfilled (more than 80%) it is not the maximum temperature that is solely important but also the differential change experienced beyond the filling temperature. If the tank were filled at a lower temperature (say 50°F) the predicted pressure of 537 psi required to rupture the tank would be realized at an aberrant fill capacity of 92-93% which could readily result from the faulty outage tube length.

References:

Pellini, W. S.; "Advances in Fracture Toughness Characterization Procedures and in Quantitative Interpretations to Fracture-Safe Design for Structural Steels." April 3, 1968; Naval Research Laboratory, Washington, D.C.

Raju, I.S., and Newman, J.C., Jr., "Stress Intensity Influence coefficients for Internal and External Surface Cracks in Cylindrical Vessels," Aspects of Fracture Mechanics in Pressure Vessels and Piping PVP Vol. 58, American Society of Mechanical Engineers, New York, New York, pages 37-48, 1978.

Report by Richard E. Caddy of the Department of Forest, State of California, dated 2-22-85, San Luis Obispo County.

Rice, J. R., "First-Order Variation in Elastic Fields Due to Variation in Location of a Planar Crack Front," Journal of Applied Mechanics, September 1985, Vol. 52.

Rolfe, S.T., and Barsom, J.M.; "Fracture and Fatigue Control in Structures" 1977 by Prentice-Hall, Inc.

"Standard for the Storage and Handling of Liquefied Petroleum Gases" 1979 edition of NFPA 58 (National Fire Protection Association Inc.)

Tada, H.; Paris, P.C.; Irwin, G.R.; "The Stress Analysis of Cracks Handbook"; Del Research Corporation, June 1973.

Vargaftik, N.B., "Tables on the Thermophysical Properties of Liquids and Gases," 2nd edition, Hemisphere Publishing Corporation.

Zahoor, A. "Closed Form Expressions for Fracture Mechanics Analyses of Cracked Pipes," Journal of Pressure Vessel Technology, Technology Briefs, May 1985, Vol. 107.

Standards and Specifications

American Association of Mechanical Engineers

ASME Boiler and Pressure Vessel Code, Section VIII, Division 1, "Rules for Construction of Unfired Vessels," 1950

ASME Boiler and Pressure Vessel Code, Section VIII, Division 1, 1983, part UG, Table of Contents

Excerpt, Table C-1, ASME Container Design, NFPA 58

American Society for Testing and Materials

ASTM A786-81 – "Standard Specifications for Rolled Steel Floor Plates"

Federal Specifications

Federal specification QQ-F-461, 1951 – "Floor Plates, Steel, Rolled"

National Fire Protection Association

NFPA 58 – Liquified Petroleum Gases," 1930s, 1947, 1949, 1979, 1986

NFPA 501C, 1982 – "Standard on Firesafety Criteria for Recreational Vehicles"

National LP-Gas Association

State Adoption of Federal Hazardous Materials and Motor Carrier Safety Regulations

Underwriters Laboratories

UL 144, 1985 – "Pressure Regulating Valves for LP-Gas"